# Photoluminescence of self-assembled InSb quantum dots grown on GaSb as a function of excitation power, temperature, and magnetic field

E. Alphandéry, R. J. Nicholas,* N. J. Mason, S. G. Lyapin, and P. C. Klipstein
*Department of Physics, Clarendon Laboratory, University of Oxford, Parks Road, Oxford OX1 3PU, United Kingdom*
(Received 9 July 2001; published 4 March 2002)

We report measurements of photoluminescence (PL) from self-assembled InSb quantum dots (QD's) grown by metal-organic vapor-phase epitaxy in a matrix of GaSb as a function of excitation power, temperature, and magnetic field. PL is observed in the region 1.7–1.8 $\mu$m from InSb quantum dots. For low excitation power the PL is dominated by the lowest quantum dot transition energy. When the excitation power is increased the quantum dot transition increases in energy by ~11 meV, and further transitions are observed from the wetting layer, bulk acceptor, and free excitons. Magneto-PL is used to calculate the in-plane dot confinement energies by fitting the data to the ground state of a Fock-Darwin set of energy levels. The in-plane confinement energy deduced increases from ~6 to ~18 meV as the excitation power is increased. This is similar to the increase in the quantum dot transition energy, and suggests that this is due to a progressive population of a distribution of strongly communicating dots with decreasing lateral sizes. Further support for this picture comes from the temperature dependence of the quantum dot transition energy, which is also found to increase by a relatively similar amount as the temperature is raised from 11 to 50 K, following a correction for the temperature dependence of the bulk energy band gaps.

DOI: 10.1103/PhysRevB.65.115322 PACS number(s): 73.21.La

## I. INTRODUCTION

Quantum dots (QD's) are three-dimensional potential wells that can trap electrons and holes and produce quantized energy levels. The density of states is a $\delta$-like function, and the electron-hole wavefunction is strongly localized. These properties have led to a surge of interest in the area of QD's. However, most of the work to data on self-assembled QD's focused on materials with band gaps in the visible region, such as the $In_xGa_{1-x}As$ on GaAs QD system.[1,2] It is therefore interesting to extend the study of QD systems to narrow-gap materials with emission in the near-infrared region, such as InSb QD's grown on GaSb as presented here. The properties of this system will be considerably different to that of an InAs/GaAs QD system, as the energy scale for QD confinement is considerably less. Our previous studies[3] showed that the difference between the wetting layer and the quantum dot transition energy is typically of order 40 meV, which is substantially smaller than the InAs case. This implies that the carriers will be much less strongly bound in InSb quantum dots, and we therefore expect them to communicate with each other down to a much lower temperature.

The successful growth of self-assembled InSb on GaSb quantum dots was demonstrated in a previous report, using the metal-organic vapor-phase epitaxy growth technique.[3] In Ref. 3, a low power photoluminescence (PL) experiment showed that InSb dots luminesce at 0.71–75 eV for a growth time larger than 2 sec, and a growth temperature ranging from 480 up to 500 °C. The optimized growth conditions were established for maximum PL intensity and a minimum full width at half maximum (FWHM) as 4 sec and 480 °C. Samples grown in these conditions gave QD peaks with a FWHM of ~15 meV, suggesting a significant dot size/composition distribution.

In this paper, we study the optimized sample more extensively. In order to confirm the existence of such a distribution in dot size and composition, and to understand the mechanism involved in the population of these dots, we perform three additional experiments. The low-power PL study of Ref. 3 is first extended into the high-power regime. The luminescence of the dots is then studied as a function of increasing temperature. Provided the binding energy of the InSb dots is small enough so that they communicate all the time, an increase in power or temperature should result in a population of progressively more confined dots with higher transition energies.

The third experiment that is carried out is a magneto-PL experiment, where the laser power is varied between 2.5 mW and 5 W and the magnetic field is applied either perpendicular to the sample surface, $\mathbf{B}_\perp$, or parallel to it, $\mathbf{B}_\parallel$. As shown in a series of previous reports, it is possible to deduce, from the variation of the dot transition energy with magnetic field, several of the dot characteristics, such as the dot in-plane confinement energies,[4] the dot lateral sizes,[4] and the dot heights.[5] In this paper, we study how these three parameters vary with increasing power. This should provide additional support for the picture of a strongly communicating dot size distribution.

## II. EXPERIMENT

The PL was excited by the 488-nm line of an argon laser operating up to a maximum power of 5 W. The light was focused at the entrance of a single 600-$\mu$m-diameter infrared fiber, which was in direct contact with the sample, cooled in liquid helium at 4 K. The signal was detected by a 77 K, cooled germanium photo detector and lock-in amplifier, and was spectrally decomposed by a HR 460 Jobin-Yvon spectrometer. The PL spectra were normalized by the response of the Ge detector. The maximum power density at the surface of the sample for a laser power of 5 W was estimated as

 ©2002 The American Physical Society

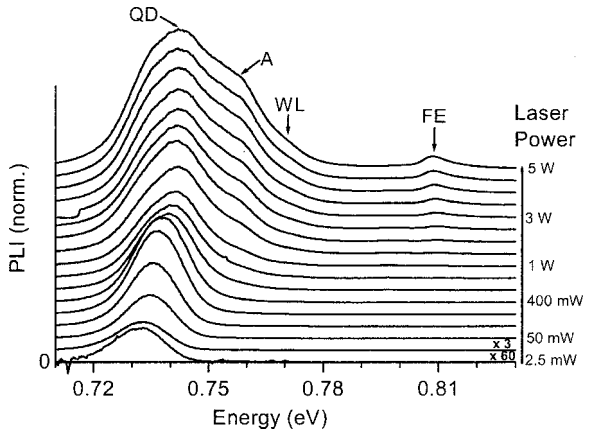


FIG. 1. The normalized PL spectra of the QD sample as a function of excitation power. The spectra are offset by 70% in the *y* direction.

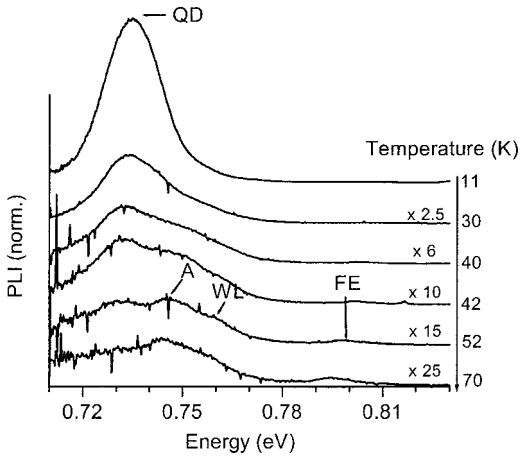


FIG. 2. The normalized PL spectra of the QD sample as a function of temperature. The spectra are offset by 70% in the *y* direction.

$\sim$186 W/cm$^2$. In order to study the luminescence as a function of temperature, the samples were placed in helium exchange gas with a laser power density of $\sim$1 W/cm$^2$, which limited the lowest temperature attained to 11 K.

The detailed growth conditions of the optimized sample, grown at 480 °C with 4 sec of InSb, were given in Ref. 3. A similar series of measurements was made on samples with two, three, and five second deposition time which gave qualitatively similar results so data in only presented for 1 sample.

## III. POWER- AND TEMPERATURE-DEPENDENT PL

In Sec. III A, we study the luminescence of the optimized sample as a function of increasing power and temperature.

### A. Description of the PL spectra

Figure 1 shows, as a function of excitation power, the PL spectra of the optimized sample. For the lowest power of 2.5 mW, the PL spectra are dominated by a low-energy peak, which was attributed to the emission of quantum dots in Ref. 3. As the excitation intensity increases, the QD feature increases in intensity, broadens, shifts up in energy, and then saturates. Once the QD feature begins to saturate, four peaks begin to appear. Two of these are attributed to bulk GaSb,[6,7] the acceptor (*A*) at 0.758 eV and a free exciton at 0.81 eV. To assign the $\sim$0.758-eV peak to the bulk acceptor, we have used the fact that its width and position were both independent of laser power (Fig. 1) and of the amount of material deposited. The fourth peak at 0.77 eV was shown to be due to the wetting layer (WL) in Ref. 3. A further increase in laser power from 1 up 5 W enhances the bulk and WL peaks very strongly.

Figure 2 shows the temperature-dependent PL spectra of the optimized sample. As the temperature is increased from 11 up 40 K the QD peak remains dominant, but its intensity strongly decreases, while for the WL and bulk acceptor peaks the PL intensity does not vary so strongly. Above 50 K, the QD, bulk acceptor, and WL peaks are of the same order of magnitude. The increase in temperature not only changes the intensity of the different peaks, but also their transition energies. As the temperature is increased, Fig. 2 shows a shift toward lower energy of the FE peak, contrasting with the behavior of the QD peak that remains at a roughly similar position.

### B. Discussion

In the first part of this section, we analyze the power-dependent PL spectra. The power dependence of the transition energy and intensities are shown in Fig. 3. The increase with power of the QD transition energy, shown in Fig. 3(a), suggests that the carriers are distributed within a rapidly communicating distribution of quantum dot sizes. At low power, the carriers are trapped in the large quantum dots with the lowest-energy states. As these quantum dots are progressively filled, electrons and holes fill smaller dots, causing the quantum dot transition energy shift toward higher energies between 2 mW and 1–2 W by $\sim$11 meV [Fig. 3(a)]. Above 1–2 W, after the whole dot size distribution has been filled, the position of the QD peak remains constant. Note that the effect of band-gap renormalization, that produces a decrease of the dot transition energy at high power in other systems,[8] does not seem to take place here. This effect is thought to be small, as there is no evidence of any decrease in energy with laser power, and excitonic interactions in this system are quite weak due to the small effective masses.

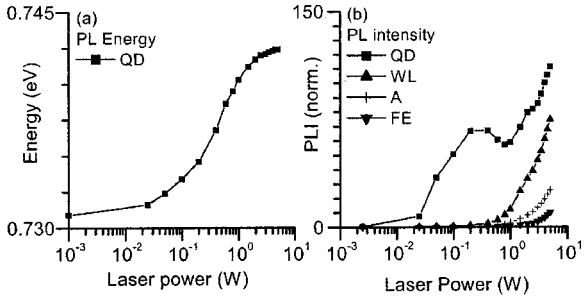


FIG. 3. (a) The QD PL energy as a function of laser power. (b) The PL intensities of the different peaks as a function of laser power.

We now turn to variations of the different peak PL intensities at relatively high pumping powers. The increase in bulk and WL PL intensities causes a decrease in QD PL intensity. The decrease occurs between 250 and 850 mW [Fig. 3(b)]. This suggests that at relatively high power carriers recombine at the bulk acceptor ($A$), a free exciton (FE), and a WL before being captured into the QD's. This behavior is consistent with the dependence on $n^2$, where $n$ is the number of excited carriers, of the bulk and WL PL intensities. In the high-power regime, where the number of excited carriers becomes large, we expect a very strong increase with power of the bulk and WL PL intensities.

From the power at which the QD PL intensity saturates, it is also possible to estimate the dot density. This power $I_s$ corresponds to a situation where the majority of the distribution of dot sizes is being filled and occurs before the contribution from the $A$, FE, and WL peaks becomes significant. Assuming that there is only one electron in each dot, the number of dots that luminesce, $N_{\mathrm{QD}}$, is equal to the saturation power $I_s$, divided by the QD emission energy $h\nu$ times the excitonic lifetime $\tau$, $N_{\mathrm{QD}}=I_s/h\nu\tau$. For an InAs/GaAs system, the QD ground state lifetime has been estimated to be 1 ns for dots with a base width of 12–14 nm,[9] while for smaller dots it has been estimated to be ~0.3 nsec.[9,10] We therefore use an average QD ground-state lifetime ($\tau$) of ~0.7 nsec. Using a saturation level of 0.1 W (calculated at half maximum) corresponding to a power density of ~4 W cm$^{-2}$ gives an estimate of the dot density as $\sim 10^{10}$ cm$^{-2}$. This is one order of magnitude larger than the $\sim 10^{9}$ cm$^{-2}$ dot density deduced by atomic force microscopy (AFM) measurements for the smallest strained dots in a 3-sec InSb sample grown at 480 °C.[3] We expect a higher density of dots for 4-sec growth and, in addition, the AFM measurements were made on an uncapped sample, and it is possible that the density of the dots is slightly lower in an uncapped sample.

We consider next the temperature dependent PL spectra of Fig. 2. We first examine the variation with temperature of the QD transition energy. We recall that an increase in temperature results in a dilatation of the lattice, a change in the band gap following the Varshni law,[11] and consequently in a decrease of the PL transition energy. This is clearly observed for the bulk free exciton in Fig. 2, where excitons are not confined. In order to examine the QD behavior, we therefore need to normalize out the band-gap shift using the Varshni formula $E_g(T)=E_g(0)-aT^2/(T+b)$, where we take $a=5.5\times10^{-4}$ eV K$^{-1}$ and $b=91$ K, which provide a good fit for the FE shift in the temperature range 4–80 K [Fig. 4(a)]. The normalized transition energy is shown in Fig. 4(a) as functions of temperature for the FE. It can be seen that a normalized FE does not vary with temperature, thus justifying the Varshni parameters used. In Fig. 4(b), we observe that the QD transition energy is increased by ~7 meV between 10 and 50 K. This suggests that as the temperature is increased, electrons and holes are thermally activated from the less confined dots, and are transferred to dots with higher confinement energies.

Considering the behavior of the carriers with decreasing temperature, we distinguish three different temperature regimes. Above ~50 K, the PL intensity of the WL peak is similar to that of the QD peak [Fig. 4(c)], which suggests that the excitons spend as much time in the WL as in the dots. This is due to the greater density of states in the WL than in the QD's. Above ~50 K, we would expect that the QD PL energy will tend towards a constant value close to the mean of the QD energy.

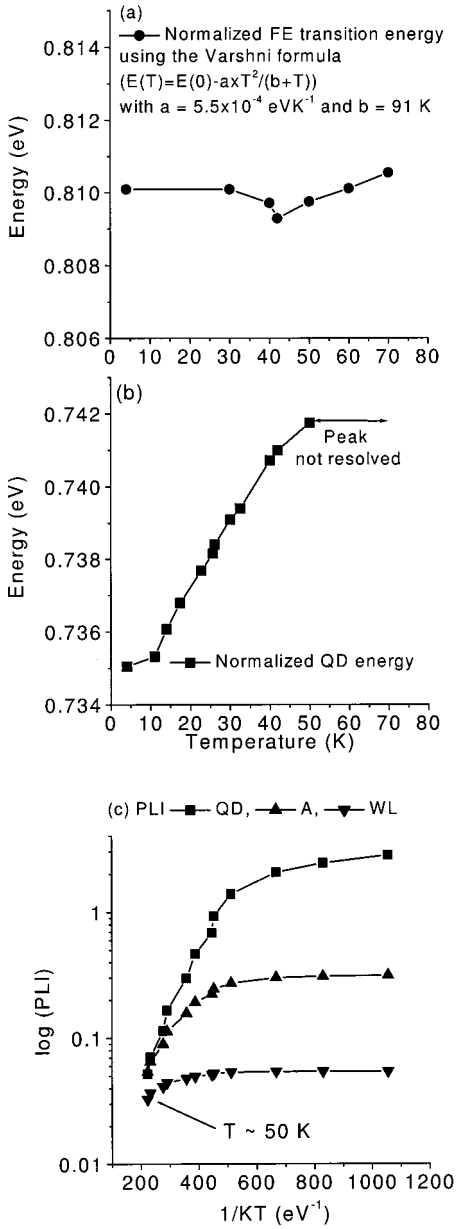


FIG. 4. (a) The normalized energy of the FE peak as a function of temperature. (b) The normalized energy of the QD peak as a function of temperature. (c) The intensities of the QD, $A$, and WL peaks as functions of temperature.

Below ~50 K the excitons begin to be localized at specific dots, but provided that the QD escape time $\tau_e$ is shorter than the recombination time $\tau_r$, they will maintain an equilibrium population, which allows them to fill the larger dots with lower energies, as shown in Fig. 4(b). During this process the mean transition energy will decrease [Fig. 4(b)]. The assumption that, at sufficiently high temperature, the escape

time is smaller than the recombination time relies on the fact that we are in the strong confinement regime, in which the recombination time is independent of temperature, $\tau_r \sim ns$, while $\tau_e$ is a decreasing function of temperature.[12]

At sufficiently low temperature the interdot communication will be suppressed as both the dot escape time lengthens and the number of dots with a lower energy falls as excitons fall deeper into the tail of the distribution of dot sizes. As a result no further change in the equilibrium population is possible. The data suggest that this occurs at ~10 K, where the shift in dot PL energy saturates and the total shift is comparable to the high temperature half width of the dot emission.

## IV. MAGNETOLUMINESCENCE

We now turn to the luminescence of the optimized sample as a function of magnetic field for a wide range of different laser powers. Two configurations of the magnetic field, either perpendicular to the sample surface, $\mathbf{B}_\perp$, or parallel to it, $\mathbf{B}_\parallel$, are studied.

### A. Description of the magneto-PL spectra

The $\mathbf{B}_\perp$ configuration is first considered. Figure 5(a) shows a series of spectra in which magnetic fields from 0 to 15 T were applied perpendicular to the surface of the sample. The laser power was kept constant at 5 W, enough to fill at 0 T the energy levels of the QD, WL and bulk acceptor. As the field is increased, the PL intensities of all these peaks are enhanced. This behavior contrasts with that observed at low power, where the WL and bulk acceptor were much less enhanced, as shown previously in Ref. 3 and in the power dependent PL spectra of Fig. 5(b).

The enhancement of the QD, bulk acceptor, and WL peaks is caused by the strong electron-hole localization induced by the reduction of the cyclotron radius,[3] which is defined by $r_c=(\hbar/eB)^{0.5}$. At low field, 0–6 T, the WL and bulk acceptor peaks are more rapidly enhanced than the QD peak. At higher field, however, the cyclotron radius eventually becomes smaller than the size of even the more strongly confined QD's. Consequently, the QD emission also becomes more probable at high field, and therefore it remains stronger than the higher-lying WL and bulk acceptor peaks.

Further evidence of the stronger confinement in the QD's comes from the smaller value of the transition energy increase with increasing field strength for the QD's, 16.4–18.9 meV, than for the bulk acceptor and WL: ~20 and ~22 meV, respectively [Fig. 5(a)]. The smaller value of the QD transition energy variation with increasing field is indeed consistent with the fact that the electron-hole wave function is localized inside the QD's, so that the QD transition energy does not increase at low field as long as the magnetic length scale remains larger than the lateral size of the dot. By contrast, the transition energies of the WL and bulk acceptor increase almost linearly with increasing field, indicating that the in-plane electron-hole wave function is not strongly localized at $B=0$ in these structures.

The power dependence is shown in Fig. 5(b) at 15 T, and can be compared with the zero-field dependence shown in Fig. 1. As the laser power is increased from 50 mW to 3 W, the QD peak initially dominates the spectra. But as the laser power is further increased from 3 to 5 W, the QD peak saturates while the WL and bulk acceptor peaks continue to increase [Fig. 5(b)]. In comparison to the behavior seen at 0 T, the bulk acceptor, WL, and QD peaks are much better resolved, and less intensity is transferred to the FE and *A* bulk peaks.

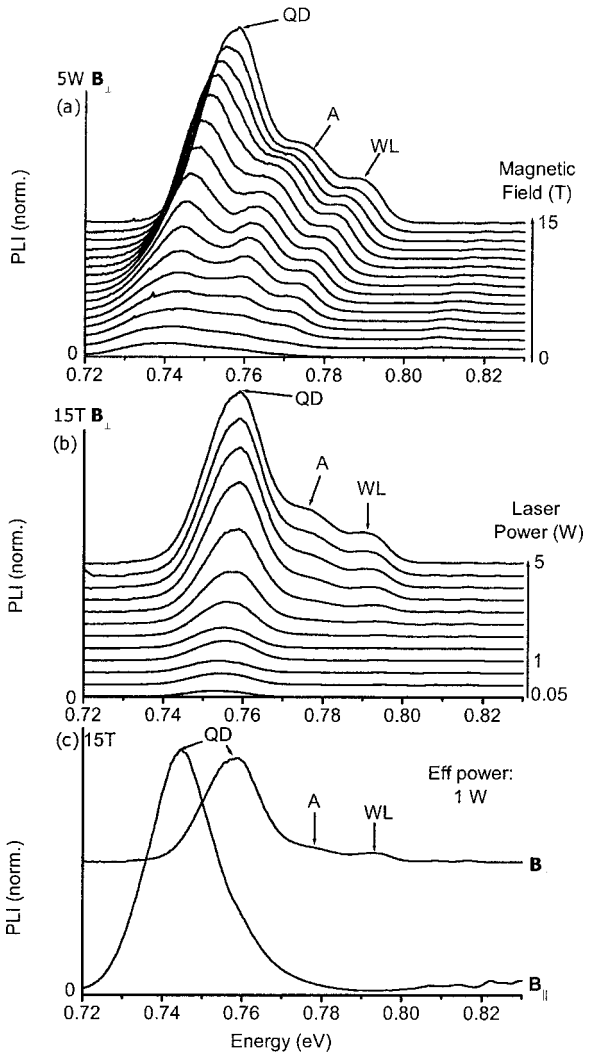


FIG. 5. (a) The normalized magneto-PL spectra, where the magnetic field is applied perpendicular to the surface of the sample $\mathbf{B}_\perp$, and varied between 0 and 15 T with 1-T increments. The laser power is kept constant at 5 W. (b) Same as in (a), with a magnetic field kept constant at 15 T and the laser power varied between 50 mW and 5 W. (c) The magneto-PL spectra in the $\mathbf{B}_\perp$ and $\mathbf{B}_\parallel$ cases for a similar power density corresponding to a laser power of 5 W in the $\mathbf{B}_\parallel$ case and of 1 W in the $\mathbf{B}_\perp$ case. In the $\mathbf{B}_\parallel$ case, the measurements were made using a small 1-mm/ 1-mm prism that reduced the excitation density by a factor of ~5. Therefore, to compare spectra with an equivalent power density, we show the 5-W $\mathbf{B}_\parallel$ spectrum with the 1-W $\mathbf{B}_\perp$ spectrum. The *y* scale is offset by 70% in (a), (b), and (c).

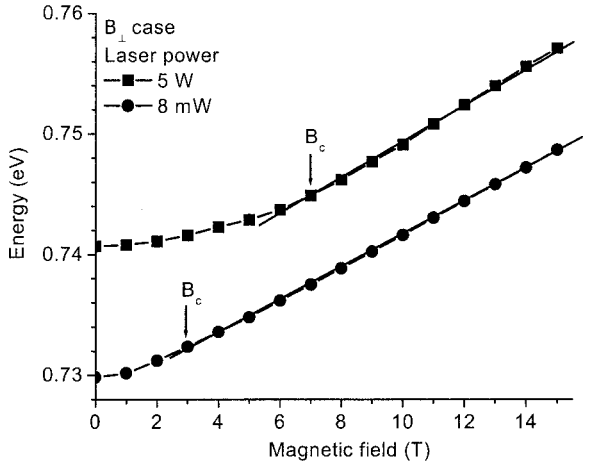


FIG. 6. The variation of the QD PL energy with magnetic field for laser powers of 8 mW and 5 W. The magnetic field is applied perpendicular to the sample surface, and varied between 0 and 15 T. $\mathbf{B}_c$ represents the field at which the transition from a diamagnetic shift to a linear variation with field occurs.

### B. Discussion

Next we turn to the quantum dots and to the process by which they are being populated with increasing power. As previously mentioned, the shift toward higher energy of the QD transition energy with increasing power suggests a strongly communicating dot size distribution, where the larger dots with the deepest potentials are being filled first before the smaller dots that have shallower potentials. The magneto-PL spectra, in the $\mathbf{B}_\perp$ configuration, provide support in several ways for the picture described above. This support relies on the different behavior of the QD peak as a function of magnetic field at low and high powers.

The variations of the QD transition energies with magnetic field are shown in Fig. 6. At low field, we observe a small diamagnetic shift of the QD transition energy, and at high field a transition to a linear variation with field. This transition occurs around the field range where $\sqrt{2}r_c$ becomes equal to the dot radius.[13] Figure 6 shows that this transition takes place at $\sim$3 and $\sim$7 T at low and high powers, respectively. Using these values of the field, we deduce that the dot diameter decreases from 40 nm at low power to 27 nm at high power. This estimate is, however, not very accurate, as the field at which the transition from a diamagnetic shift to a linear variation with field is difficult to determine.

In order to estimate the variation with power of the dot confinement energies and to obtain more accurate values of the dot lateral sizes, we have fitted the variations of the QD transition energy with field with the Fock-Darwin formula, $E_{\mathbf{B}\perp,\mathrm{exc}}=\hbar/2(4\Omega_{\mathrm{exc}}^2+\omega_c^2)^{0.5}$, where $\hbar\Omega_{\mathrm{exc}}$ is the excitonic in-plane confinement energy and $\omega_c$ is the cyclotron frequency. From this fitting, we have deduced the mean confinement energies as a function of power. Using the relation between the in-plane confinement energy and the lateral extent of the wavefunction, $\langle\rho_i^2(0)\rangle^{0.5}=(\hbar/\mu\Omega_{\mathrm{exc}})^{0.5}$, we deduce the mean dot lateral sizes as a function of laser power.

We first need to estimate the excitonic effective masses. The latter were deduced from the heavy hole effective mass of $0.34m_0$,[14] and the electron effective mass of $0.037m_0$, which was deduced from $m_e^*=m_{\mathrm{GaSb}}^*(E_{\mathrm{QD}}/E_{\mathrm{GaSb}})$, where the QD transition energy $E_{\mathrm{QD}}$ is taken to be 0.733 eV (low power). This gives a band-edge excitonic effective mass of $\sim 0.0334m_0$. Band nonparabolicity was also taken into account using the simple $\mathbf{k}\cdot\mathbf{p}$ two-band formula $m_e^*(B)=m_e^*(0)\ (1+2E/E_g)$, with $E=\omega_c/2$. The calculated effective-mass value is in good agreement with that obtained by fitting the WL transition, which gave a mean value for the fitted excitonic effective mass of $0.0333m_0$.

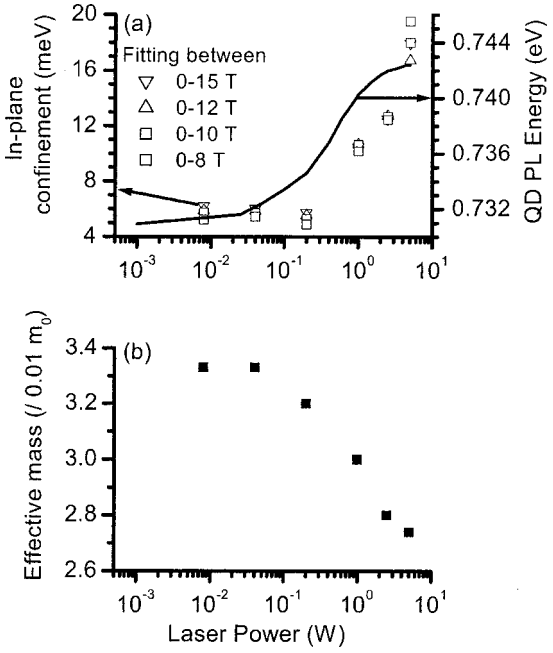


FIG. 7. (a) The in-plane and QD PL energies as a function of laser power. (b) The effective mass as a function of laser power.

Fitting the low-power excitation data at 8, and 40 mW gives good agreement with the Fock-Darwin formula using an excitonic effective mass of $\sim 0.0334m_0$, in good agreement with the expected value, and gives an in-plane QD confinement energy of $\sim 5.75\pm 1$ meV. The errors are deduced by fitting over different field ranges from 0–15, 0–12, 0–10, and 0–8 T. For higher excitation power, however, there is a substantial change in both the low-field behavior and the high-field slope of the transition energy. This means that for laser powers higher than 200 mW it is not possible to fit the data using the same values of either the effective mass or the confinement energy. Fitting between 0 and 15 T by allowing both parameters to vary showed that the confinement energy increases substantially and the excitonic effective mass falls as the excitation power increases as shown in Figs. 7(a) and 7(b). If the excitonic effective mass is constrained to remain constant at $\sim 0.0334m_0$, then the confinement energy increases to unrealistically high values and the high-field slope is not a good fit leading to a strong dependence of the fitted results on the field range used for fitting. The increase in the in-plane QD confinement energy with intensity is quite substantial, from $\sim$5.75 up to $\sim$18 meV, but the magnitude of the increase, $\sim$12 meV, is very similar to the increase of the QD transition energy with an intensity

of ~11.5 meV [Fig. 7(a)]. This provides strong support for the picture described earlier in which the shift to higher energy is associated with the population of laterally smaller and more strongly confined QD's.

As previously mentioned, it is possible to deduce the variation with power of the dot lateral sizes from the different values of the confinement energies at low and high power. We assume that the lateral extent of the in-plane electron-hole wave function, $\langle \rho_i^2(0)\rangle^{0.5}$, is equal to the dot radius. Using the values $0.033m_0$, 5.75 meV and $0.027m_0$, 18 meV for the effective masses and confinement energies at low and high power, respectively, we find that the average dot diameter decreases with power from ~40 to ~25 nm, in good agreement with our previous estimate.

The range of QD diameter corresponds to dot radii that are of the order or smaller than the effective Bohr radius of the dot material ($a_b^* \sim 27$ nm). We therefore remain in the strong confinement regime in the in-plane direction, and the electron-hole energy is quantized by the in-plane QD potential. From the values above, we deduce that the distribution of in-plane QD diameters has a variation of order ~100%, considerably more than the ~10–20 % size distribution variation established by some AFM measurements for an (In,Ga)As/GaAs QD system.[15] However, these results can not be compared directly with AFM measurements, since this measurement is only sensitive to the luminescent dots and measures over a considerable larger area ($3\times10^3$ cm$^2$). To our knowledge, this is the first time a direct estimate of the in-plane QD size distribution has been made for the luminescence emitting dots only.

Finally, we discuss the decrease in effective mass with laser power from $\sim 0.0334m_0$ (8 and 40 mW) down to $\sim 0.0274m_0$ (5 W) [Fig. 7(b)]. This may be due to several factors which are not yet possible to distinguish. The increased confinement, and possibly different indium content and strain in smaller dots may well cause a decrease of the hole effective mass.[16] Many-body effects may also lead to a decrease in mass due to either multiple population of the dots or Coulombic interactions between electrons in the dots and electrons in the WL. It should also be borne in mind that the data obtained for a laser power of 5 W is least accurate since for this power a pronounced asymmetry is observed at high field [Fig. 5(a)]. In addition, the large linewidth and overlapping WL and *A* peaks [Fig. 5(a)] make an accurate estimation of the effective mass more difficult.

For the magneto-PL spectra in the $\mathbf{B}_\parallel$ configuration [Fig. 5(c)], the enhancements of the WL and QD peaks are much smaller than seen for the $\mathbf{B}_\perp$ configuration. This suggests that as the field is increased up to 15 T, the cyclotron radius remains much larger than both the WL thickness (~2 ML) and the dot height and that the magnetic field therefore only confines the carriers in one of the in-plane directions. As shown in Fig. 8, the energy shifts of the QD peak are diamagnetic and quite small ~5. 5, and ~6 meV for laser powers of 2 mW and 5 W, respectively. The much smaller shift observed in the $\mathbf{B}_\parallel$ configuration, compared with the $\mathbf{B}_\perp$ configuration, indicates that electrons and holes are strongly confined in the growth direction at $B=0$. This is consistent with the fact that the dot height is much smaller than the lateral dot sizes. Moreover, the diamagnetic shift coefficient, which is proportional to the square of the wave function extent in the *z* direction, $\gamma = e^2\langle r_{i,z}^2\rangle/2\mu$,[5] is very similar for all powers from 2 mW to 5 W (Fig. 8), at $\sim 25.5 \pm 1.5\ \mu$eV/T$^2$, suggesting that the dot height is independent of the lateral dot size as assumed in the analysis for $\mathbf{B}_\perp$. The expression for $\gamma$ using an excitonic effective mass $\mu = (0.033-0.027)m_0$ gives an estimate of the vertical (*z*) extent of the QD wave function, $\langle r_{i,z}^2\rangle^{0.5}$, of 2.9–3 nm, in good agreement with our previous estimate.[3]

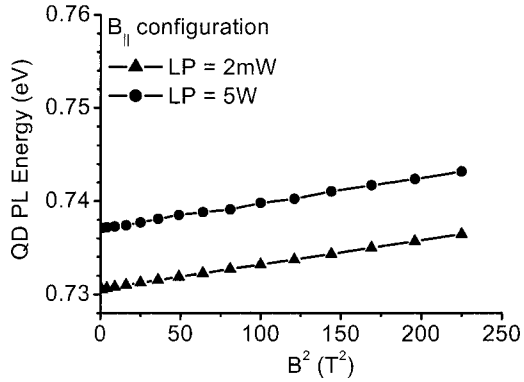


FIG. 8. The QD PL energy as a function of magnetic field for laser powers of 2 mW and 5 W in the $\mathbf{B}_\parallel$ configuration.

## V. CONCLUSION

In conclusion, we have shown that the photoluminescence of self-assembled InSb on GaSb quantum dots depends strongly on excitation intensity, temperature, and magnetic field. We have observed that the QD transition energy was shifted toward higher energy by ~7–11 meV, as the laser power and temperature were increased up to 1–2 W and 50 K respectively. This suggests that there is a large distribution of quantum dot sizes, and that dots with decreasing lateral sizes are being filled as the laser power or temperature is increased.

Applying a magnetic field perpendicular to the sample surface, $\mathbf{B}_\perp$, shifts the QD transition energies and this dependence was well fitted by the Fock-Darwin formula which allows us to deduce the in-plane QD confinement energy. The fit shows that a high pumping intensity produces an increase of the average QD transition energy by ~12 meV and a decrease in the average populated QD diameter from ~40 to ~24 nm. The change in QD confinement energy is almost exactly equal to the change in QD transition energy seen as a function of intensity. All the data are consistent with the picture that the excitons are distributed over a population of QD's with a considerable size distribution and that these dots communicate rapidly with each other down to quite low temperature.

## ACKNOWLEDGMENTS

We would like to thank I. A. Trojan from HPPI, R. Rudd from the department of materials at Oxford, and B. Zhang for useful discussions, as well as Keith Bechler and Simon Moudler for technical assistance.

*Corresponding author. Email address: r.nicholas@physics.ox.ac.uk

[1] See, for example, J-Y Marzin, J-M Gérard, A. Israël, D. Barrier, and G. Bastard, Phys. Rev. Lett. **73**, 716 (1994).

[2] For a review, see R. Nötzel, Semicond. Sci. Technol. **11**, 1365 (1996).

[3] E. Alphandéry, R. J. Nicholas, N. J. Mason, B. Zhang, P. Moëck, and G. R. Booker, Appl. Phys. Lett. **74**, 2041 (1999).

[4] See, for example, P. D. Wang, J. L. Merz, S. Fafard, R. Leon, D. Leonard, G. Medeiros-Ribeiro, M. Oestreich, P. M. Petroff, K. Uchida, N. Miura, H. Akiyama and H. Sakaki, Phys. Rev. B **53**, 16 458 (1996).

[5] S. N. Walck and T. L. Reinecke, Phys. Rev. B **57**, 9088 (1998).

[6] M. Lee, D. J. Nicholas, K. E. Singer, and B. Hamilton, J. Appl. Phys. **59**, 2895 (1986).

[7] E. T. R. Chidley, S. K. Haywood, A. B. Henriques, N. J. Mason, R. J. Nicholas, and P. J. Walker, Semicond. Sci. Technol. **6**, 45 (1991).

[8] Z. L. Yuan, E. R. A. D. Foo, J. F. Ryan, D. J. Mowbray, M. S. Skolnick, and M. Hopkinson, Physica B **272**, 12 (1999).

[9] D. Bimberg, M. Grundmann, and N. N. Ledenstov, *Quantum Dot Heterostructures* (Wiley, Chichester, 1999), p. 251.

[10] M. Grundmann, N. N. Ledenstov, J. Chriten, J. Böhrer, D. Bimberg, S. S. Ruvimov, P. Werner, U. Richter, U. Gössele, J. Heydenreich, V. M. Ustinov, A. Y. Egorov, A. E. Zhukov, P. S. Kop'ev and Z. I. Alferov, Phys. Status Solidi B **188**, 249 (1995).

[11] Y. P. Varshni, Physica (Amsterdam) **34**, 149 (1967).

[12] D. Bimberg, M. Grundmann, and N. N. Ledenstov, *Quantum Dot Heterostructures* (Ref. 9), p. 156.

[13] M. Hayne, R. Provoost, M. K. Zundel, Y. M. Manz, K. Eberl and V. V. Moschalkov, Phys. Rev. B **62**, 10 324 (2000).

[14] G. Harbeke, O. Madelung, and U. Rössler, in *Semiconductors, Physics of Group IV and Elements and III–V Compounds*, edited by K. Hellwege and O. Madelung, Landolt-Bernstein, New Series, Group III, Vol. 17, Pt. a (Springer-Verlag, Würzburg, 1982), p. 262.

[15] See, for example, S. Ruvimov, P. Werner, K. Scheerschmidt, U. Gösele, J. Heydenreich, U. Richter, N. N. Ledenstov, M. Grundmann, D. Bimberg, V. M. Ustinov, A. Yu. Egorov, P. S. Kop'ev, and Zh. I. Alferov, Phys. Rev. B **51,** 14766 (1995).

[16] A. Ghiti and E. P. O'Reilly, Semicond. Sci. Technol. **8**, 1655 (1993).